

Serine/threonine phosphatase 5 (PP5C/PPP5C) regulates the ISOC channel through a PP5C-FKBP5I axis

Caleb L. Hamilton^{1,2}, Kevin A. Abney¹, Audrey A. Vasauskas³, Mikhail Alexeyev^{2,4}, Li Ni¹, Richard E. Honkanen¹, Jonathan G. Scammell⁵ and Donna L. Cioffi^{1,2}

¹Department of Biochemistry and Molecular Biology, University of South Alabama, Mobile, AL, USA; ²Center for Lung Biology, University of South Alabama, Mobile, AL, USA; ³Department of Anatomical Sciences and Molecular Medicine, Alabama College of Osteopathic Medicine, Dothan, AL, USA; ⁴Department of Physiology and Cell Biology, University of South Alabama, Mobile, AL, USA; ⁵Department of Comparative Medicine, University of South Alabama, Mobile, AL, USA

Abstract

Pulmonary endothelial cells express a store-operated calcium entry current (I_{SOC}), which contributes to inter-endothelial cell gap formation. I_{SOC} is regulated by a heterocomplex of proteins that includes the immunophilin FKBP5I. FKBP5I inhibits I_{SOC} by mechanisms that are not fully understood. In pulmonary artery endothelial cells (PAECs) we have shown that FKBP5I increases microtubule polymerization, an event that is critical for I_{SOC} inhibition by FKBP5I. In neurons, FKBP5I promotes microtubule stability through facilitation of tau dephosphorylation. However, FKBP5I does not possess phosphatase activity. Protein phosphatase 5 (PP5C/PPP5C) can dephosphorylate tau, and similar to FKBP5I, PP5C possesses tetratricopeptide repeats (TPR) that mediate interaction with heat shock protein-90 (HSP90) chaperone/scaffolding complexes. We therefore tested whether PP5C contributes to FKBP5I-mediated inhibition of I_{SOC} . Both siRNA-mediated suppression of PP5C expression in PAECs and genetic disruption of PP5C in HEK293 cells attenuate FKBP5I-mediated inhibition of I_{SOC} . Reintroduction of catalytically competent, but not catalytically inactive PP5C, restored FKBP5I-mediated inhibition of I_{SOC} . PAEC cell fractionation studies identified both PP5C and the ISOC heterocomplex in the same membrane fractions. Further, PP5C co-precipitates with TRPC4, an essential subunit of ISOC channel. Finally, to determine if PP5C is required for FKBP5I-mediated inhibition of calcium entry-induced inter-endothelial cell gap formation, we measured gap area by wide-field microscopy and performed biotin gap quantification assay and electric cell-substrate impedance sensing (ECIS[®]). Collectively, the data presented indicate that suppression of PP5C expression negates the protective effect of FKBP5I. These observations identify PP5C as a novel member of the ISOC heterocomplex that is required for FKBP5I-mediated inhibition of I_{SOC} .

Keywords

phosphatase, PP5C, FKBP5I, ISOC calcium channel, endothelial barrier

Date received: 29 September 2017; accepted: 19 December 2017

Pulmonary Circulation 2018; 8(1) 1–12

DOI: 10.1177/2045893217753156

Disruption of the endothelial monolayer leads to increased vascular permeability, increasing deposition of fluid, solutes, and macromolecules into perivascular tissue. Specifically, inter-endothelial cell gap formation is one mechanism of endothelial dysfunction that contributes to increased permeability in the pulmonary circulation.¹ Increases in cytosolic calcium contribute to inter-endothelial cell gap formation in pulmonary endothelial cells,² and transient receptor

potential canonical (TRPC) proteins contribute to increased cytosolic calcium through mediating calcium entry.³ TRPC4 and TRPC1 are necessary for the calcium conductance of

Corresponding author:

Donna L. Cioffi, MSB 2316, Department of Biochemistry and Molecular Biology, 5851 USA Drive N., University of South Alabama Mobile, AL 36688, USA.

Email: dlcioffi@southalabama.edu



Creative Commons Non Commercial CC-BY-NC: This article is distributed under the terms of the Creative

Commons Attribution-NonCommercial 4.0 License (<http://www.creativecommons.org/licenses/by-nc/4.0/>)

which permits non-commercial use, reproduction and distribution of the work without further permission provided the original work is attributed as specified on the SAGE and Open Access pages (<https://us.sagepub.com/en-us/nam/open-access-at-sage>).

© The Author(s) 2018.

Reprints and permissions:

sagepub.co.uk/journalsPermissions.nav

journals.sagepub.com/home/pul



the moderately calcium-selective current, I_{soc} , a small inwardly rectifying current with a reversal potential around +32 mV.^{4,5} Additionally, I_{soc} is a thapsigargin-activated current. When activated, I_{soc} leads to inter-endothelial cell gap formation within the pulmonary circulation.⁶

Our laboratory has shown that a large molecular weight immunophilin, FKBP51, is part of the ISOC heterocomplex. Furthermore, we have shown that FKBP51 regulates calcium entry in pulmonary artery endothelial cells (PAECs).⁷ FKBP51 inhibits thapsigargin-induced I_{soc} in both PAECs and HEK293 cells, without affecting other thapsigargin-induced calcium entry pathways. This suggests that FKBP51 is a specific inhibitor of I_{soc} . However, the mechanism by which FKBP51 regulates I_{soc} is poorly understood. FKBP51 promotes microtubule polymerization in neurons through dephosphorylation events of microtubule-associated proteins⁸ and we have recently demonstrated that inhibition of I_{soc} by FKBP51 is dependent upon an FKBP51-mediated increase in microtubule polymerization.⁹ However, because FKBP51 lacks phosphatase activity the link between FKBP51 and dephosphorylation remains unknown. Serine/threonine protein phosphatase five (PP5C; encoded by *PPP5C*) dephosphorylates microtubule-associated proteins in neurons.¹⁰ Thus, we investigated the role of PP5C in ISOC function and tested to determine if PP5C plays a role in FKBP51-mediated inhibition of I_{soc} .

We found that neither the suppression nor genetic disruption of PP5C expression significantly altered thapsigargin-induced I_{soc} ; however, without PP5C FKBP51-mediated inhibition of I_{soc} was abolished. Reintroduction of wild-type (WT) PP5C, but not catalytically deficient PP5C, to PP5C^{-/-} cells restored the FKBP51-mediated inhibition of I_{soc} . Further, a subpopulation of PP5C localizes and interacts with the ISOC heterocomplex. Since the inhibition of I_{soc} by FKBP51 leads to reduced inter-endothelial cell gap formation,⁹ and we observed that PP5C is required for the FKBP51-mediated inhibition of I_{soc} , we next investigated the role of PP5C in inter-endothelial cell gap formation. Indeed, the FKBP51-mediated protection of the endothelial barrier against calcium entry-induced gap formation was lost upon PP5C small interfering RNA (siRNA) treatment. Cumulatively, our observations reveal a novel role for PP5C in ion channel regulation and endothelial barrier function.

Materials and methods

Reagents

All reagents were obtained from Sigma–Aldrich (St. Louis, MO, USA) unless otherwise indicated. Cell culture medium was obtained from Thermo Fisher Scientific (Waltham, MA, USA) or Santa Cruz Biotechnology (Santa Cruz, CA, USA). Penicillin/streptomycin was obtained from Thermo Fisher Scientific. Fetal bovine serum (FBS) was purchased from Thermo Fisher Scientific. EquafETAL[®]

bovine serum (EBS) was purchased from Atlas Biologicals, Inc. (Fort Collins, CO, USA). Hank's Balanced Salt Solution (HBSS) was purchased from Thermo Fisher Scientific. Monoclonal antibodies to FKBP51 were described previously.¹¹ TRPC4 antibody was obtained from Alomone Labs (Jerusalem, Israel). Polyclonal antibody for PP5C was previously described.¹² β -actin antibody was purchased from Santa Cruz Biotechnology.

Cell culture

PAECs were isolated from Sprague-Dawley rats as previously described.¹³ Cell culture media of PAECs and HEK293 cells contained high glucose DMEM supplemented with 10% FBS or EBS, penicillin G (50 U/mL), and streptomycin (0.05 mg/mL). All animal work was approved by the University of South Alabama Institutional Animal Care and Use Committee in compliance with the National Institutes of Health *Guide for the Care and Use of Laboratory Animals*.

Western blotting

Cell lysis was achieved by scraping and sonification (10 s at 12% output; Branson Digital Sonifier model S-450D; Branson, Danbury, CT, USA) in RIPA buffer (Boston BioProducts; Ashland, MA, USA) with 1% protease inhibitor cocktail. Whole cell lysates were centrifuged at 12,000 × g for 20 min. Lysates were electrophoresed on 4–12% bis-Tris gels (Thermo Fisher Scientific) and proteins transferred to nitrocellulose membranes at 100 V. Membranes were blocked for 1 h with milk (5% non-fat dry milk/0.2% BSA in PBS supplemented with 0.1% Tween-20) at room temperature. Membranes were then incubated with primary antibodies overnight at 4°C and with secondary antibodies for 1 h at room temperature. The dilutions for primary antibodies were as follows: 1:700 for FKBP51 and 1:1000 for TRPC4, PP5C and β -Actin. Dilutions for secondary antibodies were: 1:5000 anti-mouse for FKBP51, 1:30,000 anti-mouse for β -actin, and 1:10,000 anti-rabbit for PP5C and TRPC4. Protein visualization was achieved with Supersignal West Pico or West Femto chemiluminescent substrates (Thermo Fisher Scientific). Densitometry of visualized westerns was achieved using Image J software.¹⁵

Genetic suppression of PP5C expression with siRNA

The suppression of PP5C expression was achieved with siRNA targeted to the sequence

5'-AATGGCGATGGCGGAGGGCGA-3' (Qiagen; Hilden, Germany). Transfection of PAECs was initiated when monolayers had obtained 50–60% confluence. PAEC monolayers were transfected with a 20 nM final siRNA concentration in lipofectamine 3000 (Thermo Fisher Scientific). Complete cell culture media was added to the transfected monolayers at 4 h and siRNA incubation continued to 48 h.

Construction of PP5C expression plasmid

Complementary DNA (cDNA) comprising the complete coding region of human PP5C¹⁶ was subcloned into pBlueScript (Stratagene; San Diego, CA, USA; Genbank X52328). A prokaryotic expression vector was constructed by polymerase chain reaction (PCR) amplification with primers incorporating a 5' EcoRI restriction site, a methionine start codon followed by a sequence encoding a hexahistidine affinity tag (MGGHHHHHHG; his-tag), and a 3' PstI restriction site. The amplified fragment was subcloned into pKK223-3 (Pharmacia; New York City, NY, USA; Genbank M77749). A peptide NLYFQGA (which forms a part of a Tobacco Etch Virus [TEV] protease recognition sequence) was added to the N-terminal and subcloned into pMalc2E (New England Biolabs; Ipswich, MA, USA; NEB #N8066) using conventional methods. Expression constructs with the indicated mutations were made using a QuikChange Site-Directed Mutagenesis Kit (Stratagene). These expression constructs encoded an N-terminal Maltose Binding Protein (MBP) fusion with the catalytic domain of PP5C (residue Ser169 to residue Met499; designated PP5C), plus a linker sequence (MGGHHHHHHG SVVDSLDIENLYFQGA) between the fusion partners containing a hexahistidine affinity tag, a spacer sequence, and a TEV protease cleavage site. The N-terminal MBP aids the folding of PP5C when expressed in *E. coli* and the His-tag aids purification. Primer sequences used in the generation of these constructs are provided in Supplementary Table 1. Following purification, the MBP and hexahistidine tags were removed by treatment with TEV protease. The catalytically active proteins were then further purified using ion exchange (monoQ; Pharmacia) chromatography. Additional details are described in Ni et al.¹⁷

Phosphatase assays

Protein phosphatase activity was measured by the dephosphorylation of DiFMUP in assay buffer (50 mM MOPS, 5 mM β -ME, 1 mM MnCl_2) according to established methods.^{16–18}

PP5C^{-/-} and PP5C catalytically inactive cell lines

Disruption of PP5C expression in HEK293 cells was achieved using CRISPR/Cas9-mediated cleavage of exon one, adapting essentially the same strategy used to generate PP5C knockout mice.¹⁹ Briefly, following the X-tremeGENE protocol, HEK293 cells were transfected with 1 μg of a Cas9 expressing plasmid into which a RNA-guide template targeting PP5C was subcloned after the U6-promoter (Addgene; Cambridge, MA, USA; #42230) and allowed to grow for three days. On day 3 using flow cytometry, cells were individually sorted into 96 well plates. The clonally derived cell lines were then screened using western analysis to identify lines with no PP5C protein. Genomic DNA sequencing was used to validate the

disruption of PP5C expression, which occurred due to stochastic insertion that induces frame shift.

Reintroduction of WT (PP5C-WT) and catalytically inactive (PP5C-Cat Δ) expression constructs. Human PP5C was amplified by PCR incorporating EcoRI and NotI sites by adding the appropriate sequence into the synthetic primers. The construct was then subcloned into pcDNA3. Plasmids allowing the expression of cDNA encoding PP5C (WT) were transfected into PP5C^{-/-} cells with X-tremeGENE (0.5 μg) for 24 h following the manufacturer's protocol. To generate catalytically inactive PP5C, we performed a comprehensive site-directed mutagenesis of PP5C, in which all ten of conserved amino acids within the catalytic site identified by the high-resolution crystal structure of PP5C¹⁶ were systematically mutated using Stratagene QuikChange II Site-Directed Mutagenesis. Oligonucleotide sequences used for the introduction of the mutations are provided in Supplementary Table 2. All plasmids were sequenced to verify the fidelity of the constructs. Each of the mutant forms of PP5C were then subcloned into pKK223-3. After assessing purity via SDS-PAGE and Coomassie blue staining (Supplementary Fig. 1), the purified proteins were tested for phosphatase activity using identical buffers and substrates, as described for WT PP5C above. His304 was confirmed as the proton donor in the catalytic mechanism and the catalytically inactive construct (PP5C-H304N) subcloned into P-lenti6-V5-D-topo (Addgene). Catalytically dead PP5C (PP5C-Cat Δ) or WT PP5C was then reintroduced into HEK293 PP5C^{-/-} cell line as described previously.²⁰ Following blastomycin selection, expression of the reintroduced constructs was confirmed by western analysis.

Overexpression of FKBP51 in PAECs

Production of lentivirus encoding human FKBP51 (lv3899) and stable transduction of PAECs were as previously described.⁹ For acute overexpression of FKBP51, HEK293 cells, and PAECs were treated with a 1:1 ratio of cell culture media and lv3899 in the presence of polybrene (8 $\mu\text{g}/\text{mL}$) for 24 h and cells were subjected to patch clamp electrophysiology or lysis for western blot analysis after the 24-h lentiviral infection.

Patch-clamp electrophysiology

Cells were seeded onto glass coverslips and grown to confluence in 35-mm dishes. Patch-clamp electrophysiology recordings were performed in whole-cell configuration on electrically isolated cells as described.^{7,14} Non-enzymatic cell dissociation solution in PBS (Sigma, cat. no. C5789) was utilized for the isolation of single cells. Transmembrane current evoked by step depolarization in 20 mV increments in the range of -100 to $+80$ mV was measured with an Axopatch 200B Amplifier (Molecular Devices; Sunnyvale, CA, USA). PClamp10 software was used to measure current as the mean value of the current amplitude during the last

20 ms of each step. Standard pipette and bath solutions were composed as previously described,⁷ and all solutions were adjusted to 290–300 mOsm/L with sucrose. Hemo capillaries (A-M Systems; Sequim, WA, USA) were pulled by a micro-pipette puller (P-97; Sutter Instruments; Novato, CA, USA) to produce recording pipettes. Pipettes were heat-polished by a microforge (MF-830; Narishige; Tokyo, Japan) and filled with standard pipette solution to a final resistance of 3–5 megaohms. All experiments were performed at room temperature. Representative patch tracings are shown for each newly introduced cell type in the respective figure corresponding to the current-voltage (IV) plot in which electrophysiological recordings of the cell line are first depicted. Representative tracings are indicative of the electrical recording of one cell within the corresponding IV plot. Patch tracings for subsequent treatments of the cell lines are shown in the supplemental material (Supplementary Fig. 2).

Membrane-cytoskeletal preparation

Cell fractionation of PAECs was performed in the cold room (4°C) using the membrane-cytoskeletal preparation as previously described.¹⁴ PAEC lysates were pelleted and re-suspended in ice-cold sucrose buffer and homogenized with a dounce homogenizer. The homogenate was centrifuged at 3000 × g (17 min, 4°C) and the supernatant collected. The supernatant was subsequently centrifuged at 50,000 × g (30 min, 4°C). The pellet was re-suspended in octyl-D-glucopyranoside containing extraction buffer with potassium iodide (KI). Samples were incubated for 40 min in the cold room and centrifuged at 145,000 × g (50 min, 4°C). The membrane containing supernatant was collected and the cytoskeletal containing pellet was solubilized with sonication.

Co-precipitations

Co-precipitation of TRPC4 with PP5C was achieved with SureBeads™ IgG conjugated magnetic beads (Bio-Rad; Hercules, CA, USA) following manufacturer's instructions. Following a 10 min incubation of the magnetic beads with the precipitating antibody, whole cell lysates of PAECs were incubated with the beads for 1 h under agitation. After washing, protein was eluted from the beads with 40 uL of 1 × Laemlli buffer (diluted from 6 × Laemlli buffer; Boston BioProducts, Ashland, MA, USA) for 10 min at 70°C.

Wide-field gap formation studies

PAECs were seeded onto 35-mm coverslips and grown to confluence. PAEC monolayers were imaged (20×) at 15 s intervals for 2 min using a Zeiss Observer.D1 wide-field microscope and AxioVision Rel 4.8 Software. Thapsigargin (1 μM) was then added and monolayers imaged for 30 min. Cell gap size was measured by outlining gap areas and using the pixel-to-micron conversion feature of the AxioVision Rel 4.8 Software.

Biotin gap assay

Protocol was performed as previously described.²¹ PAECs were grown to confluence in biotin-coated plates (Thermo Fisher Scientific; PI15151). Control PAECs were treated with either vehicle (ethanol, 0.05%) or dexamethasone (10 nM) for 48 h. To activate calcium entry-induced gap formation, cells were treated with thapsigargin (1 μM) for a total of 10 min, or DMSO (0.05%). Seven minutes after thapsigargin treatment, cells were incubated with streptavidin-488 (5 μg/mL) for 3 min. Monolayers were then washed twice with PBS (200 μL/well). A final volume of 100 μL PBS was added to each well and fluorescence of biotin-conjugated streptavidin-488 was measured on a BioTek (Winooski, VT) Synergy 2 plate reader and the data were recorded with BioTek Gen5 software.

Electric cell-substrate impedance sensing (ECIS®)

ECIS® experiments were performed as previously described.²² A stable baseline resistance was recorded for at least 30 min before administration of thapsigargin (1 μM). Resistance changes were recorded until a new constant baseline was established.

Statistical analysis

GraphPad version 5.0 software (San Diego, CA, USA) was utilized for statistical analysis. A two-way ANOVA and Bonferroni post hoc test was used to assess comparisons between multiple groups. Data are presented as mean ± SEM and values were considered significantly different when $P < 0.05$.

Results

PP5C is required for the FKBP51-mediated inhibition of I_{soc}

The moderately calcium-selective I_{soc} is activated by the plant alkaloid thapsigargin, which results in depletion of endoplasmic reticulum stores through inhibition of the sarcoplasmic/endoplasmic reticular Ca^{2+} /ATPase.²³ We have previously shown that two immunophilins, FKBP51 and FKBP52, regulate thapsigargin-induced calcium entry.⁷ Calcium entry through I_{soc} is inhibited by FKBP51 overexpression in both HEK293 cells and PAECs via a mechanism dependent upon increased microtubule polymerization.^{7,9} FKBP51 has been implicated in promoting microtubule polymerization through the isomerization and dephosphorylation of tau.⁸ Since FKBP51 lacks phosphatase activity, a phosphatase must be involved, and PP5C is a phosphatase reported to dephosphorylate tau.¹⁰ Like FKBP51, PP5C contains TPR domains through which it interacts with HSP90.²⁴ We therefore wanted to study the role of PP5C in the FKBP51-mediated inhibition of I_{soc} .

FKBP51 overexpression was achieved by lentiviral transduction of human FKBP51 in HEK293 cells (Fig. 1a, b). Consistent with our previous observations in PAECs,⁷ FKBP51 overexpression significantly inhibited I_{soc} in HEK293 cells (Fig. 1c). To determine whether PP5C is required for the inhibition of I_{soc} by FKBP51, FKBP51 was over-expressed in HEK293 cells in which PP5C expression was genetically disrupted. Although FKBP51 over-expression inhibited I_{soc} in control HEK293 cells, over-expression of FKBP51 was unable to inhibit I_{soc} in the PP5C^{-/-} cells (Fig. 1d–f). Reintroduction of full-length PP5C into PP5C^{-/-} cells restored the FKBP51-mediated inhibition of I_{soc} .

The catalytic activity of PP5C is required for the FKBP51-mediated inhibition of I_{soc}

We have previously reported the high-resolution (1.6 Å) crystal structure of PP5C in complex with phosphate (mimicking the leaving group phosphate; PDB code 1S95), which allowed us to define the PP5C catalytic mechanism.¹⁶ The PP5C active-site comprises ten amino acids—D²⁴², XH²⁴⁴(X)_{26–27}, D²⁷¹, XXD²⁷⁴, R²⁷⁵(X)₂₈, N³⁰³, H³⁰⁴(X)₄₈, H³⁵²(X)_{48–54}, R⁴⁰⁰, (X)₂₇, H⁴²⁷—that are 100% conserved in PP1C, PP2AC, and PP2BC, which share the same catalytic mechanism. Six of the conserved active site amino acids act as metal-coordinating residues (Asp²⁴², His²⁴⁴, Asp²⁷¹,

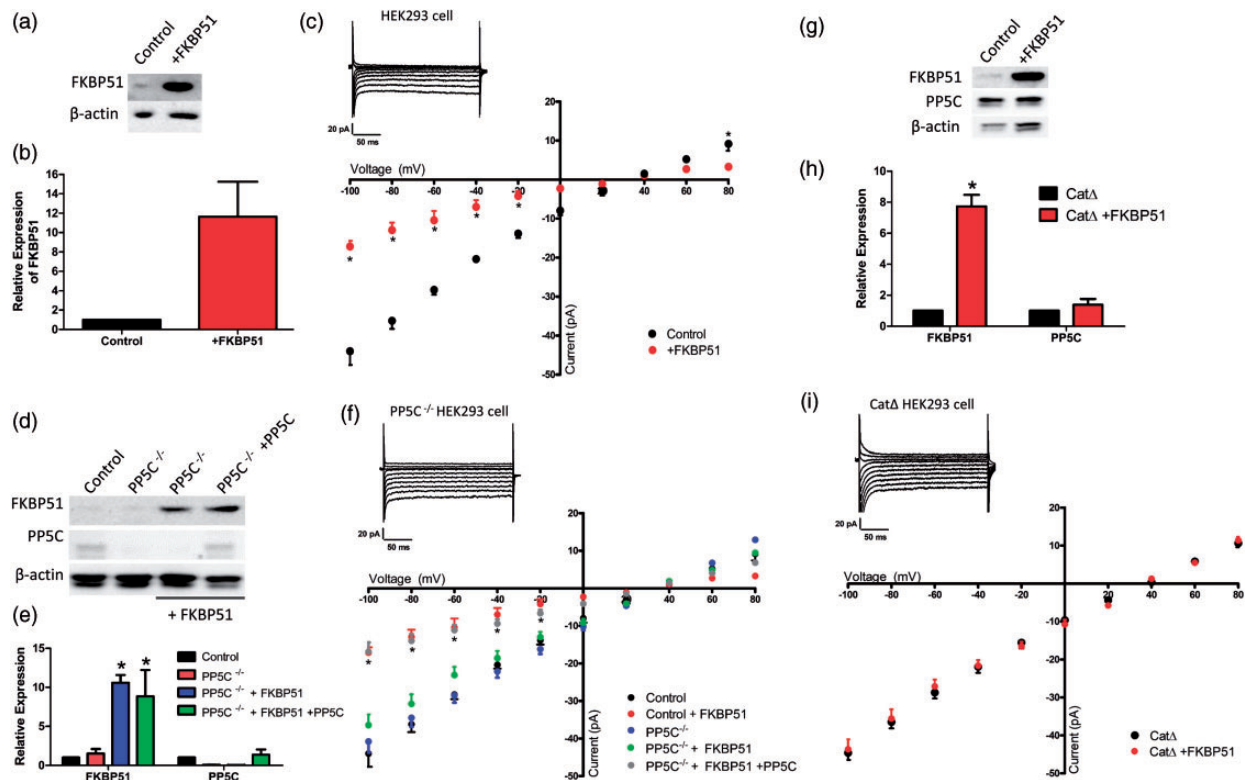


Fig. 1. PP5C is required for the FKBP51-mediated inhibition of I_{soc} in HEK293 cells. (a) Western blot analysis and (b) densitometry (calculated as band intensity of FKBP51 relative to that of β -actin and normalized to one for control HEK293 cells) analysis reveal that lentiviral transduction of hFKBP51 resulted in acute FKBP51 overexpression in control HEK293 cells ($n = 3$). (c) Thapsigargin-induced I_{soc} was recorded using whole-cell patch clamp electrophysiology. Overexpression of FKBP51 (red) resulted in significantly decreased I_{soc} compared to control HEK293 cells (black) at the indicated testing potentials. $*P < 0.05$ control vs. FKBP51 overexpressing HEK293 cells; $n = 6$. (d) Western blot analysis and (e) densitometry (calculated as band intensity of the indicated protein relative to that of β -actin and normalized to one for control HEK293 cells) confirm the disruption of PP5C disruption (PP5C^{-/-}) utilizing CRISPR/Cas9. Lentiviral transduction of hFKBP51 resulted in overexpression of FKBP51 in PP5C^{-/-} cells, and in PP5C^{-/-} cells in which PP5C was reintroduced. $*P < 0.05$ vs. control; $n = 3$. (f) Overexpression of FKBP51 did not inhibit I_{soc} in PP5C^{-/-} cells (green). Reintroduction of PP5C into cells restored the FKBP51-mediated inhibition of I_{soc} (gray). Data for control (black) and FKBP51 overexpressing cells (red) are those shown in (c) and are included here for comparison. (g) Catalytic-deficient PP5C was reintroduced into the PP5C^{-/-} cells (PP5C- Δ Cat). An acute overexpression of hFKBP51 was achieved by lentiviral transduction of the PP5C- Δ Cat HEK293 cells as shown by western blot and (h) by densitometry (calculated as band intensity of the indicated protein relative to that of β -actin and normalized to one for control PP5C- Δ Cat HEK293 cells). $*P < 0.05$ vs. Cat Δ ; $n = 3$. (i) Overexpression of FKBP51 in PP5C- Δ Cat cells (red) did not inhibit I_{soc} relative to control PP5C- Δ Cat HEK293 cells (black) ($n = 6$).

Table 1. Kinetic parameters of PP5C and PP5C mutants.

	k_{cat} (S^{-1})	K_{M} (μM)	$k_{\text{cat}}/K_{\text{M}}$ ($\text{M}^{-1} \text{S}^{-1}$)	Relative $k_{\text{cat}}/K_{\text{M}}$ (%)
PP5CWT	9.9 ± 0.4	133.4 ± 10.5	74,212	100
D242N	5.1 ± 0.7	119.0 ± 28.5	42,857	57.75
H244Q	0.019 ± 0.004	392.1 ± 120.1	48	0.06
D271N	2.4 ± 0.5	144.0 ± 52.5	16,666	22.46
D274N	0.038 ± 0.005	77.7 ± 23.9	489	0.66
R275K	0.40 ± 0.04	71.7 ± 20.4	5579	7.52
N303D	0.019 ± 0.004	477.2 ± 127.9	40	0.05
H304Q	0.029 ± 0.002	311.5 ± 37.5	93	0.13
R400K	0.44 ± 0.02	37.3 ± 4.7	11,796	15.90
H427Q	0.062 ± 0.008	89.8 ± 25.9	690	0.93
Y451F	20.2 ± 3.2	352.0 ± 79.8	57,386	77.33

The data shown are the mean \pm SD; $n = 3$; for additional detail see supplemental data.

Asn³⁰³, His³⁵², and His⁴²⁷) and four (Arg²⁷⁵, Asn³⁰³, His³⁰⁴, and Arg⁴⁰⁰) position the phosphate ion through strong hydrogen bonds to the phosphoryl oxygens of the substrate (Supplementary Fig. 3). The structure of the PP5C catalytic domain with bound phosphate provided a model of substrate-enzyme interactions in a near attack configuration. Analysis of the substrate analog complex revealed that His³⁰⁴ forms a short (2.6 Å), strong hydrogen bond with O⁴ of phosphate (the substrate leaving group oxygen). Asp²⁷⁴ hydrogen bonds with the imidazole of His³⁰⁴ (increasing the imidazole pKa). This stabilizes the histidine side chain in a cationic state that is capable of protonating the leaving group. Thus, His³⁰⁴ acts as a general acid in the hydrolysis reaction.¹⁶ In addition, positively charged His³⁰⁴, along with Arg²⁷⁵ and Arg⁴⁰⁰, contribute to electrostatic stabilization of the transition state by neutralization of the negative charge developing on the leaving group oxygen. Therefore, mutation of His³⁰⁴, Asp²⁷⁴, or the key metal coordinating amino acids were predicted to generate a catalytic inactive enzyme.

To validate the proposed catalytic mechanism and to determine the best amino acid to mutate in order to generate a catalytically inactive enzyme, we performed a comprehensive site-directed mutagenesis of PP5C, in which all the conserved amino acids within the catalytic site were systematically mutated (Supplementary Fig. 4). Each mutant form of PP5C was then expressed and highly purified using methods developed for the production and characterization of PP5C (Supplementary Fig. 1).¹⁷ Steady-state kinetic analysis was then performed on PP5C and each of the 11 mutants using a well-established substrate, DiFMUP,¹⁷ and identical assay conditions. As seen from the kinetic data (Table 1), mutations affecting metal coordinating residues (e.g. His244, Asp271, Asn303, and His427) or the proton donor (His304) essentially ablates catalytic activity.

To determine whether the catalytic activity of PP5C is required for the FKBP51-mediated inhibition of I_{soc} , vectors were generated in which His304 was replaced with asparagine (H304N) or glutamate (H304Q) to produce variants with essentially no catalytic activity (PP5C-CatΔ). We then reintroduced PP5C-CatΔ into the HEK293 cell line in which we previously used CRISPR/Cas9 to disrupt PP5C expression. In the PP5C-CatΔ cells, FKBP51 overexpression was unable to inhibit I_{soc} (Fig. 1i) indicating that the phosphatase activity of PP5C is needed for the FKBP51-mediated inhibition of I_{soc} . However, as shown above (Fig. 1f), when native PP5C was reintroduced, FKBP51 mediated inhibition of I_{soc} was restored. Together, these observations indicate that PP5C catalytic activity is needed for the FKBP51-mediated inhibition of I_{soc} .

PP5C is also required for the FKBP51-mediated inhibition of I_{soc} in PAECs

PAECs and HEK293 cells express similar I_{soc} electrophysiology.⁷ However, because mechanisms of I_{soc} regulation are so poorly understood it was essential to verify PP5C is also needed for the FKBP51-mediated inhibition of I_{soc} in PAECs before exploring physiological significance. To address this, we increased FKBP51 expression using two independent methods and decreased PP5C expression using siRNA. We first utilized dexamethasone (Dex) to increase the expression of FKBP51 in PAECs (Fig. 2a, b), which our laboratory previously showed inhibits I_{soc} in PAECs.⁷ To verify that the inhibition of I_{soc} was due to FKBP51 and not off-target effects of dexamethasone or glucocorticoid signaling, a PAEC line was generated to constitutively overexpress FKBP51 (cFKBP51 Fig. 2d, e).⁹ Dexamethasone treatment (Fig. 2c) and constitutive FKBP51 overexpression (Fig. 2f) both significantly inhibited I_{soc} in PAECs in the presence of scrambled siRNA. In contrast, the inhibition of I_{soc} by Dex (Fig. 2c) or with FKBP51 overexpression (Fig. 2f) was negated with even a modest decrease in PP5C expression by siRNA. These data confirm that PP5C contributes to the FKBP51-mediated inhibition of I_{soc} in PAECs.

PP5C associates with the ISOC channel heterocomplex

The ISOC channel heterocomplex comprises both channel pore-forming proteins and proteins that associate with the intracellular N- and C-terminal domains of the channel proteins. A spectrin-protein 4.1-TRPC4 interaction is required for the activation of I_{soc} in PAECs,^{4,14} and TRPC4 knockout mice do not express I_{soc} .²⁵ These observations indicate that TRPC4 is an essential channel protein in the ISOC heterocomplex. Our laboratory has also shown that the cochaperones FKBP51 and FKBP52 co-precipitate with TRPC4 in PAECs.⁷ As FKBP51 has been shown to serve as a scaffold independent of HSP90 for serine/threonine

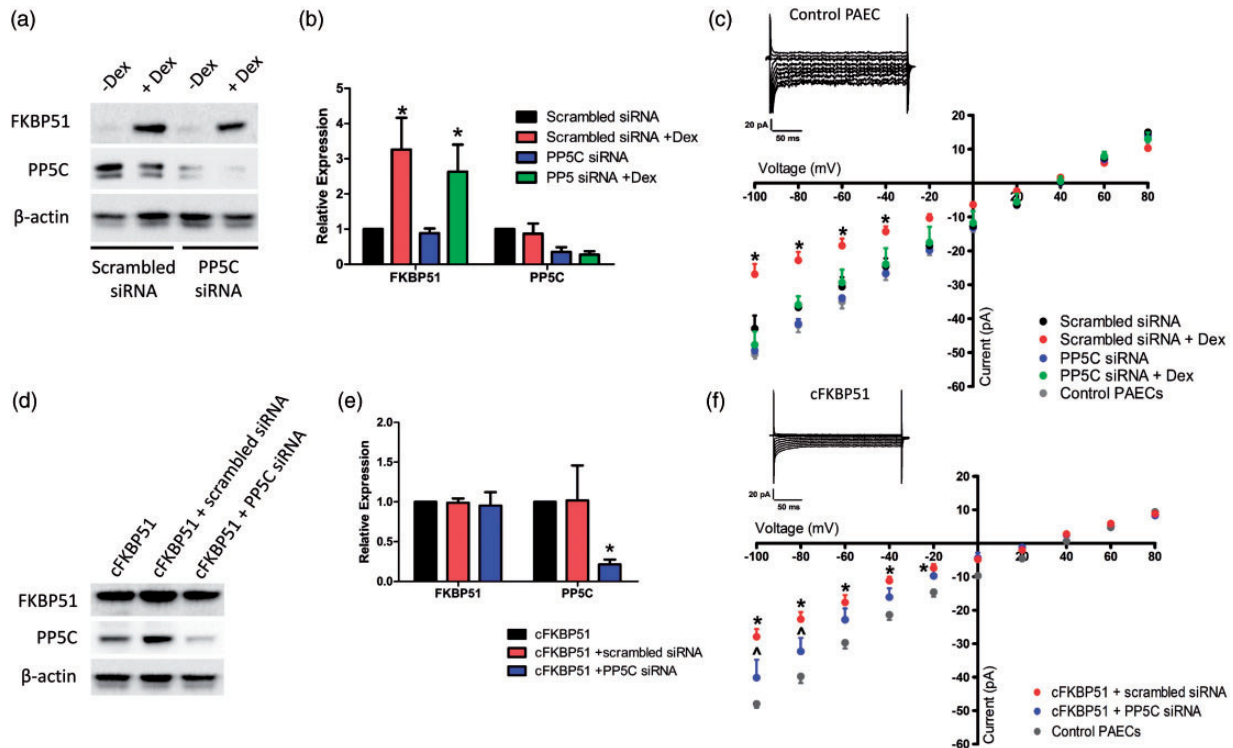


Fig. 2. PP5C is required for the FKBP51-mediated inhibition of I_{soc} in PAECs. (a) Genetic suppression of PP5C expression was achieved by 48 h siRNA transfection of PAECs. As analyzed by western blot and (b) densitometry (calculated as band intensity of the indicated protein relative to that of β -actin and normalized to one for control PAECs), dexamethasone (Dex; 10 nM) treatment resulted in the overexpression of FKBP51 in PAECs transfected with PP5C siRNA or a scrambled control. $*P < 0.05$ vs. no Dex treatment; $n = 3$. (c) I_{soc} in Dex (10 nM)-treated PAECs (red) was significantly decreased from control PAECs (gray). PP5C siRNA in PAECs expressing endogenous FKBP51 (vehicle control) did not change I_{soc} , but in PAECs expressing increased FKBP51, genetic suppression of PP5C prevented inhibition of I_{soc} ($*P < 0.05$; $n = 6$). (d) PP5C siRNA treatment decreases PP5C expression in constitutive FKBP51 overexpressing PAECs (cFKBP51) as shown by western blot analysis and (e) densitometry (calculated as band intensity of the indicated protein relative to that of β -actin and normalized to one for control cFKBP51 PAECs. $*P < 0.05$ vs. scrambled siRNA; $n = 3$). (f) cFKBP51 cells treated with scrambled siRNA (red) demonstrated reduced I_{soc} relative to control PAECs (gray) ($*P < 0.05$; $n = 5$). FKBP51 overexpressing PAECs treated with PP5C siRNA (blue) resulted in significantly increased I_{soc} compared to scrambled control (red) ($*P < 0.05$; $n = 5$). cFKBP51 cells treated with PP5C siRNA (blue) do not have a significantly different I_{soc} than control PAECs (gray). Data for control PAECs (gray) are those shown in (c) and are included here for comparison.

phosphatases,^{26,27} we wanted to determine whether PP5C also associates with TRPC4 of the ISOC heterocomplex.

We first tested to determine whether PP5C is found in plasma membranes where the ISOC channel is localized. To detect PP5C in cell membranes of PAECs, a membrane-cytoskeletal preparation was utilized to isolate TRPC4-containing membrane fractions of PAECs.¹⁴ We observed that some PP5C is located in the TRPC4-containing membrane fraction of PAECs (Fig. 3a). The cytoskeletal protein actin was resolved only in the cytoskeletal fraction. To address whether PP5C associates with TRPC4 in PAECs, co-precipitations were performed (Fig. 3b). PP5C co-precipitated with TRPC4 in PAECs and reciprocally, TRPC4 co-precipitated with PP5C. Co-precipitation of PP5C and TRPC4 was also observed in HEK293 cells (data not shown). Collectively, these data reveal that a population of PP5C resides at the plasma membrane and interacts with the ISOC channel.

Suppression of PP5C expression attenuates the FKBP51-mediated inhibition of calcium entry-induced inter-endothelial cell gap formation

Activation of I_{soc} contributes to inter-endothelial cell gap formation in endothelial cells of the pulmonary circulation.⁶ We have recently shown that FKBP51-mediated inhibition of I_{soc} is sufficient to decrease calcium-induced inter-endothelial cell gap formation in PAECs.⁹ Having demonstrated that PP5C is required for the FKBP51-mediated inhibition of I_{soc} , we wanted to determine whether PP5C plays a biological role needed for the protective effect of FKBP51 on the endothelial barrier. In these studies, dexamethasone or lentiviral infection were used to increase the expression of FKBP51, and siRNA was used to decrease PP5C expression. We then measured thapsigargin-induced inter-endothelial cell gap formation in confluent PAECs using wide-field microscopy. In the presence of scrambled

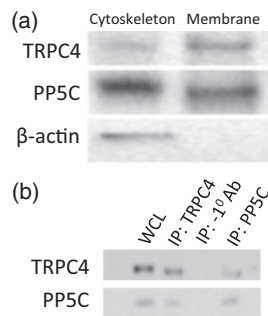


Fig. 3. PP5C associates with TRPC4 in PAECs. (a) A membrane fractionation assay was utilized to determine whether PP5C is located at the membrane of PAECs. Indeed, a population of PP5C is located at the cell membrane of PAECs where TRPC4 and the ISOC hetero-complex are located. This image is representative of $n = 4$. (b) To determine if PP5C associates with TRPC4 in whole cell lysates of PAECs, immunoprecipitations were performed with IgG-conjugated magnetic SureBeads™. PP5C co-precipitated with TRPC4. Reciprocally, TRPC4 co-precipitated upon immunoprecipitation of PP5C. WCL, whole cell lysate. Control samples were prepared in absence of primary antibody (IP: -IgG Ab). The image is representative of $n = 3$.

siRNA, FKBP51 overexpression resulted in significant decreased gap area 10 min following thapsigargin treatment compared to control PAECs (Fig. 4a). In PAECs treated with PP5C siRNA without FKBP51 overexpression, gap formation was comparable to control cells. To determine whether PP5C is needed for the FKBP51-mediated inhibition of inter-endothelial cell gap formation in PAECs, suppression of PP5C expression with siRNA was again utilized. PP5C suppression attenuated the dexamethasone-mediated inhibition of gap formation, and significantly increased gap formation in the constitutive FKBP51 overexpressing PAECs (Supplementary Fig. 5). Due to the substantial difference in initial gap area between groups, relative area is depicted in which initial gap area at $t = 0$ min is normalized to 1 for each group (Fig. 4b). Normalization of gap area reveals a significant increase in inter-endothelial cell gap formation due to PP5C siRNA-treated PAECs in which FKBP51 was overexpressed.

To confirm that PP5C is needed for the FKBP51-mediated inhibition of inter-endothelial cell gap formation, and ensure our observations are not subject to bias due to the inherent subjectivity of wide-field gap measurements, a 96-well fluorescent assay to assess gap formation first described by Dubrovskiy et al. was utilized. In this assay, gap formation is assessed by quantifying fluorescence of streptavidin bound to the basal surface of biotin-coated wells revealed by inter-endothelial cell gap formation.²¹ Fluorescence increased in control PAECs following thapsigargin treatment but did not increase in FKBP51 overexpressing cells treated with scrambled siRNA (Fig. 4c). However, in PP5C siRNA-treated FKBP51-overexpressing PAECs fluorescence increased following thapsigargin treatment. These observations validate observations made by

wide-field microscopy, confirming a role for PP5C in the suppression of FKBP51 mediated inter-endothelial cell gap formation.

To further validate our observations, changes in endothelial monolayer resistance were assessed using ECIS®. Treatment of control PAECs with thapsigargin resulted in a transient decrease in monolayer resistance, indicative of an increase in endothelial gap formation. In dexamethasone-treated (Fig. 5a–c) and constitutive FKBP51 overexpressing PAECs (Fig. 5d–f) the decrease in resistance following thapsigargin treatment was attenuated compared to control PAECs, which is consistent with FKBP51's protective role in inter-endothelial cell gap formation. In the presence of PP5C siRNA, both dexamethasone treatment and FKBP51 overexpressing endothelial cells exhibited increased thapsigargin-induced resistance loss compared to the respective scrambled siRNA controls. However, in the constitutive FKBP51 overexpressing PAECs treated with PP5C siRNA, the thapsigargin-induced resistance loss was not transient, as resistance decline was observed through the rest of the experiment. While the exact mechanisms that contribute to the persistent resistance loss are unknown, we have observed that the cFKBP51 PAECs have a more extensive microtubule network than control PAECs.⁹ While the increased microtubule stability in cFKBP51 PAECs likely contributes to a protective role against inter-endothelial cell gap formation,²⁸ the PP5C siRNA-treated cFKBP51 cells may lack the microtubule dynamics needed to reseal endothelial cell gaps effectively. Nevertheless, as suppression of PP5C expression attenuated the protective role of FKBP51 on endothelial resistance loss in the constitutive FKBP51 overexpressing PAECs and the dexamethasone treated PAECs, the data confirm that PP5C is indeed needed for the FKBP51-mediated inhibition of calcium entry-induced inter-endothelial cell gap formation.

Discussion

Activation of the endothelial I_{soc} leads to inter-endothelial cell gap formation, which increases vascular permeability in the pulmonary circulation.⁶ Our laboratory has shown that moderate increases in expression of FKBP51 inhibits I_{soc} and protects the endothelium from calcium entry-induced disruption.^{7,9} However, upregulation of FKBP51 may not be an effective therapeutic strategy against endothelial barrier disruption as it is also a potent inhibitor of glucocorticoid receptor (GR) signaling.^{11,29} GRs regulate many cellular functions through their regulation of nuclear transcription factors.^{30–32} Specifically, nuclear translocation of GR and the resulting transcriptional regulation are needed for the downregulation of inflammatory cytokines.^{31,33} As many instances of inter-endothelial cell gap formation are initiated by inflammatory events, such as in atherosclerosis and acute respiratory distress syndrome, the ability of GR to suppress inflammatory cytokines in the endothelium is essential to maintain homeostasis.

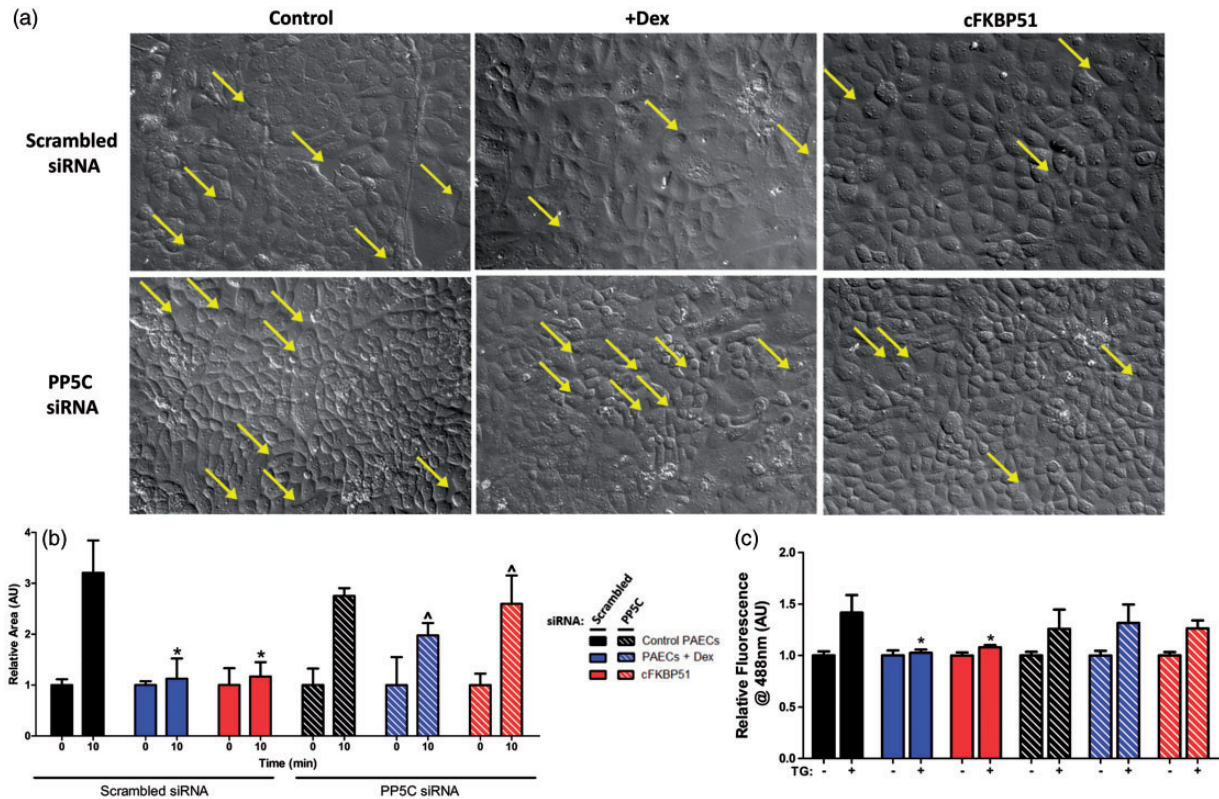


Fig. 4. PP5C is needed for the FKBP51-mediated inhibition of calcium entry-induced inter-endothelial cell gap formation. Thapsigargin (1 μ M) was used to initiate calcium entry and downstream inter-endothelial cell gap formation. (a–c) Wide-field microscopy was used to assess inter-endothelial cell gap formation in confluent PAECs. (a) Representative images at 10 min following thapsigargin treatment are shown. Yellow arrows indicate inter-endothelial cell gaps. (b) Gaps were measured with AxioVision Rel 4.8 Software and due to the substantial difference in initial gap area between groups, relative area is also depicted in which initial gap area at $t = 0$ min is normalized to 1 for each group. FKBP51 overexpression with dexamethasone (Dex; 10 nM; blue solid) and constitutive overexpression (cFKBP51; red solid) significantly inhibited total gap area relative to control PAECs treated with scrambled siRNA (black solid). PP5C siRNA-treated PAECs (black stripes) did not demonstrate significantly different gap area compared to scrambled siRNA controls (black solid). $*P < 0.05$; $n = 3$. PP5C siRNA treated PAECs in which Dex was used to overexpress FKBP51 (blue stripes) did not result in significantly altered gap area relative to control PAECs (black solid). However, PP5C siRNA treated PAECs in which Dex was used to overexpress FKBP51 (blue stripes) did have significantly greater gap area compared to Dex treated PAECs in the presence of scrambled siRNA (blue solid). $^{\wedge}P < 0.05$; $n = 3$. PP5C siRNA treatment in cFKBP51 cells (red stripes) resulted in significantly increased gap area compared to scrambled siRNA-treated cFKBP51 cells. $^{\wedge}P < 0.05$; $n = 3$. Relative gap formation was not significantly different between control PAECs and cFKBP51 cells treated with PP5C siRNA. (c) Gap formation was also assessed with a biotin-coated 96-well assay. Confluent PAECs were treated with either thapsigargin (+) or DMSO (–) for 10 min. Streptavidin-488 was added to the biotin-coated wells and gap formation assessed by the total fluorescence of the streptavidin bound to the plate. FKBP51 overexpression with Dex (10 nM; blue solid) demonstrated significantly less fluorescence upon thapsigargin treatment than control PAECs (black solid). cFKBP51 cells (red solid) also demonstrated decreased fluorescence compared to control PAECs. In Dex-treated and cFKBP51 cells in which expression of PP5C was suppressed with siRNA, there was no inhibition of thapsigargin-induced fluorescence as compared to control PAECs. $*P < 0.05$; $n = 14$.

However, when FKBP51 is present in mature GR it prevents the translocation of GR to the nucleus thus inhibiting GR-mediated transcription.³⁴ Therefore, it is essential that we unravel the mechanisms by which FKBP51 inhibits I_{soc} to optimize its efficacy in inflammatory diseases.

In this study, we identify PP5C as a novel member of the ISOC heterocomplex that is required for inhibitory action of FKBP51 on both thapsigargin-induced I_{soc} and inter-endothelial cell gap formation. PP5C is a serine/threonine phosphatase that is known to interact with other proteins via its N-terminal TPR domains.³⁵ FKBP51 has a similar TPR domain, and the TPR domains of PP5C and FKBP51

dynamically compete for a consensus binding to HSP90 within mature GRs.²⁴ Through this interaction, PP5C also regulates GR activity in cells via mechanisms that are independent of its catalytic activity. Like FKBP51, most studies indicate that PP5C is a negative regulator of GR signaling. Specifically, Zou et al. demonstrated that siRNA-mediated suppression of PP5C expression resulted in an increase in basal and dexamethasone-stimulated GR activity in A549 lung carcinoma cells.³⁶ Furthermore, it has been determined that dephosphorylation of GR by PP5C at Ser211 inhibits GR translocation into the nuclei in MCF-7 cells.³⁷ Dephosphorylation of Ser211 by PP5C has also been

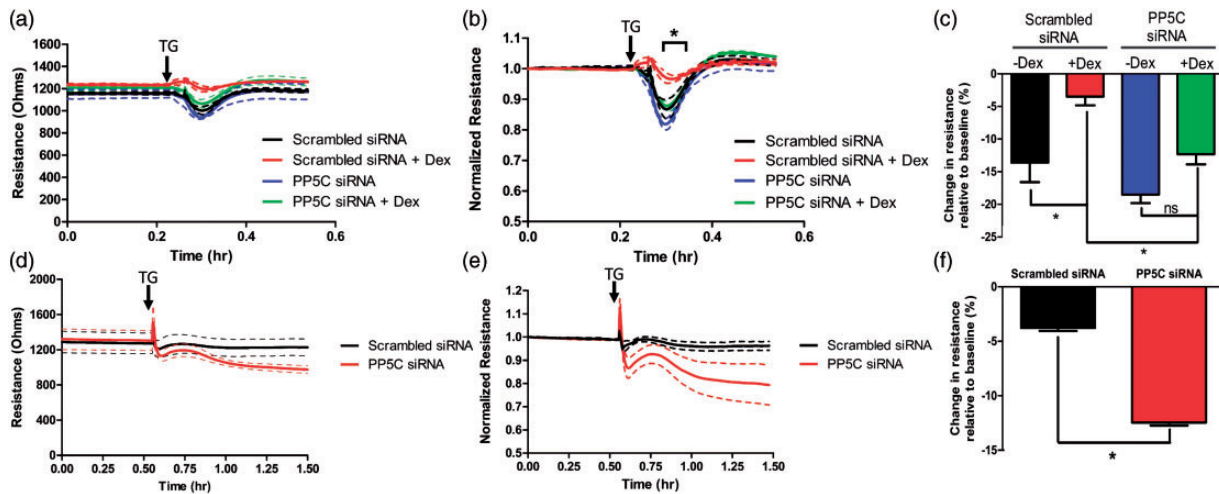


Fig. 5. PP5C is required for the FKBP51-mediated inhibition of trans-endothelial resistance loss. ECIS[®] was used to measure trans-endothelial resistance in confluent PAECs. Thapsigargin (1 μ M) was used to initiate calcium entry and downstream resistance loss in PAECs. (a, d) Total resistance; (b, e) normalized resistance. (a–c) Dexamethasone (Dex; 10 nM; red) treatment reduced trans-endothelial resistance loss compared to control PAECs (black) in the presence of scrambled siRNA. Neither the PP5C siRNA-treated PAECs treated with Dex or DMSO vehicle (0.05%) resulted in significantly reduced resistance loss relative to control PAECs. (b) The bracket shows the range at which Dex-treated PAECs demonstrate significantly greater resistance compared to control PAECs. * P < 0.05 by two-way ANOVA; n = 3. (c) Dex treatment significantly decreased the peak trans-endothelial resistance loss relative to baseline in the presence of scrambled siRNA but not in the presence of PP5C siRNA. * P < 0.05 by students t -test; n = 3. (d, e) Suppression of PP5C expression with siRNA treatment of constitutive FKBP51 overexpressing PAECs (cFKBP51; red) resulted in greater trans-endothelial resistance loss relative to scrambled siRNA-treated cFKBP51 cells (black). (f) PP5C siRNA-treated cFKBP51 cells demonstrated significantly greater peak trans-endothelial resistance decrease relative to baseline compared to cFKBP51 cells treated with scrambled siRNA. * P < 0.05 by Student's t -test; n = 7.

shown to inhibit steroid responsiveness and GR activity in airway smooth muscle cells.³⁸ Together, these findings indicate that PP5C possesses similar pharmacological limitations to FKBP51 as a standalone treatment of inflammatory-mediated endothelial barrier disruption, as both PP5C and FKBP51 are negative regulators of GR.

Despite the inhibitory roles of FKBP51 and PP5C on GR activity, the PP5C-FKBP51 axis remains a promising pharmacologic target in the regulation of I_{soc} and inter-endothelial cell gap formation. Specifically, as FKBP51 is such a highly GR-regulated protein that infers glucocorticoid resistance, it would be beneficial to determine how to prime the FKBP51-mediated inhibition of I_{soc} without altering expression levels of FKBP51. As PP5C is essential for the effect of FKBP51 on I_{soc} , targeted activation of PP5C may allow for the optimization of the FKBP51-mediated inhibition of I_{soc} . Our current study shows that a population of PP5C resides at the membrane of PAECs where it interacts with the ISOC heterocomplex. Chatterjee et al. demonstrated that the TPR domain of PP5C binds to Rac1 GTPase, which when activated, increases the translocation of PP5C to HeLa cell membranes.³⁹ As GR resides in the cytosolic and nuclear fractions of cells, increasing the translocation of PP5C to the plasma membrane could allow for an increase in the FKBP51-mediated inhibition of I_{soc} without analogous inhibitory effects of GR. As other serine/threonine phosphatases including PP2A have been shown to serve a protective role in endothelial junctions,⁴⁰ it is

possible that PP5C also would serve a similar effect if a larger population was present at the membrane.

In addition to promoting translocation of PP5C to the plasma membrane as a potential therapeutic strategy, many physiological activators of PP5C have been identified. Ramsey et al. identified that long-chain fatty acyl-CoA esters and the C-terminal domain of HSP90 increase substrate access to the catalytic domain of purified PP5C.⁴¹ Furthermore, Yamaguchi et al. demonstrated that members of the S100 protein family greatly increase the activity of PP5C in COS-7 cells in a calcium-dependent manner.⁴² As calcium entry through the ISOC channel results in inter-endothelial cell gap formation, S100 proteins may serve as novel targets in the calcium-dependent activation of PP5C and protection against calcium-mediated gap formation. Unfortunately, while much progress has been made in the development of specific pharmacologic inhibitors of PP5C, little work has been dedicated to developing PP5C agonists.

Lastly, as FKBP51 and PP5C both mediate their effects in neurons via dephosphorylation of the microtubule-associated protein tau,^{8,10} it is possible that the effect of PP5C on the FKBP51-mediated inhibition of I_{soc} may be microtubule-dependent. Endothelial cells of the pulmonary circulation express many microtubule associated proteins, including tau.⁴³ As microtubule stabilization with taxol has been shown to inhibit I_{soc} in pulmonary microvascular endothelial cells,⁵ it is possible that FKBP51 and PP5C may be working together to dephosphorylate tau

resulting in increased microtubule stability in PAECs. Indeed, we observed an increase in microtubule stability in FKBP51 overexpressing PAECs and demonstrated that this increased microtubule stability was critical for the FKBP51-mediated inhibition of I_{SOC} .⁹ Future studies will determine if PP5C is required for the FKBP51-mediated promotion of microtubule stability and tau dephosphorylation in PAECs.

Collectively, our observations demonstrate that PP5C associates with the ISOC heterocomplex and is required for the FKBP51-mediated inhibition of I_{SOC} and interendothelial cell gap formation. The data indicate specifically that the catalytic activity of PP5C is important for the FKBP51-mediated inhibition of I_{SOC} . Future studies will be directed towards better understanding the mechanisms by which PP5C regulates FKBP51 function.

Acknowledgements

The authors would like to thank Linn Ayers and Anna Buford for endothelial cell isolation and culture.

Funding

This work was supported by NIH R01HL107778 and NIH T32HL076125.

Conflict of Interest

None declared.

References

- Patterson CE, Stasek JE, Schaphorst KL, et al. Mechanisms of pertussis toxin-induced barrier dysfunction in bovine pulmonary artery endothelial cell monolayers. *Am J Physiol* 1995; 268: L926–934.
- Cioffi DL, Moore TM, Schaack J, et al. Dominant regulation of interendothelial cell gap formation by Ca^{2+} -inhibited type 6 adenylyl cyclase. *J Cell Biol* 2002; 157: 1267–1278.
- Cioffi DL, Lowe K, Alvarez DF, et al. TRPing on the lung endothelium: Ca^{2+} channels that regulate barrier function. *Antioxid Redox Signal* 2009; 11: 765–776.
- Wu S, Sangerman J, Li M, et al. Essential control of an endothelial cell I_{SOC} by the spectrin membrane skeleton. *J Cell Biol* 2001; 154: 1225–1234.
- Wu S, Chen H, Alexeyev MF, et al. Microtubule motors regulate I_{SOC} activation necessary to increase endothelial cell permeability. *J Biol Chem* 2007; 282: 34801–34808.
- Wu S, Cioffi EA, Alvarez D, et al. Essential role of a Ca^{2+} -selective, store-operated current (I_{SOC}) in endothelial cell permeability: determinants of the vascular leak site. *Circ Res* 2005; 96: 856–863.
- Kadeba PI, Vasauskas AA, Chen H, et al. Regulation of store-operated Ca^{2+} entry by FK506-binding immunophilins. *Cell Calcium* 2013; 53: 275–285.
- Jinwal UK, Koren J III, Borysov SI, et al. The Hsp90 co-chaperone, FKBP51, increases tau stability and polymerizes microtubules. *J Neurosci* 2010; 30: 591–599.
- Hamilton CL, Kadeba PI, Vasauskas AA, et al. Protective role of FKBP51 in calcium entry-induced endothelial barrier disruption. *Pulm Circ* 2018; 8(1).
- Liu F, Iqbal K, Grundke-Iqbal I, et al. Dephosphorylation of tau by protein phosphatase 5: impairment in Alzheimer's disease. *J Biol Chem* 2004; 280: 1790–1796.
- Reynolds PD, Ruan Y, Smith DF, et al. Glucocorticoid resistance in the squirrel monkey is associated with overexpression of the immunophilin FKBP51. *J Clin Endocrinol Metab* 1999; 84: 663–669.
- Zuo Z, Dean NM and Honkanen RE. Serine/threonine protein phosphatase type 5 acts upstream of p53 to regulate the induction of p21(WAF1/Cip1) and mediate growth arrest. *J Biol Chem* 1998; 273: 12250–12258.
- Kelly JJ, Moore TM, Babal P, et al. Pulmonary microvascular and macrovascular endothelial cells: differential regulation of Ca^{2+} and permeability. *Am J Physiol* 1998; 274: L810–819.
- Cioffi DL, Wu S, Alexeyev M, et al. Activation of the endothelial store-operated I_{SOC} Ca^{2+} channel requires interaction of protein 4.1 with TRPC4. *Circ Res* 2005; 97: 1164–1172.
- Schneider CA, Rasband WS and Eliceiri KW. NIH Image to ImageJ: 25 years of image analysis. *Nat Methods* 2012; 9: 671–675.
- Swingle MR, Honkanen RE and Cizak EM. Structural basis for the catalytic activity of human serine/threonine protein phosphatase-5. *J Biol Chem* 2004; 279: 33992–33999.
- Ni L, Swingle MS, Bourgeois AC, et al. High yield expression of serine/threonine protein phosphatase type 5, and a fluorescent assay suitable for use in the detection of catalytic inhibitors. *Assay Drug Dev Technol* 2007; 5: 645–653.
- Chattopadhyay D, Swingle MR, Salter EA, et al. Crystal structures and mutagenesis of PPP-family ser/thr protein phosphatases elucidate the selectivity of cantharidin and novel norcantharidin-based inhibitors of PP5C. *Biochem Pharmacol* 2016; 109: 14–26.
- Amable L, Grankvist N, Largen JW, et al. Disruption of serine/threonine protein phosphatase 5 (PP5:PPP5C) in mice reveals a novel role for PP5 in the regulation of ultraviolet light-induced phosphorylation of serine/threonine protein kinase Chk1 (CHEK1). *J Biol Chem* 2011; 286: 40413–40422.
- Skarra DV, Goudreault M, Choi H, et al. Label-free quantitative proteomics and SAINT analysis enable interactome mapping for the human Ser/Thr protein phosphatase 5. *Proteomics* 2011; 11: 1508–1516.
- Dubrovskiy O, Birukova AA and Birukov KG. Measurement of local permeability at subcellular level in cell models of agonist- and ventilator-induced lung injury. *Lab Invest* 2013; 93: 254–263.
- Cioffi DL, Pandey S, Alvarez DF, et al. Terminal sialic acids are an important determinant of pulmonary endothelial barrier integrity. *Am J Physiol Lung Cell Mol Physiol* 2012; 302: L1067–1077.
- Thastrup O, Cullen PJ, Drobak BK, et al. Thapsigargin, a tumor promoter, discharges intracellular Ca^{2+} stores by specific inhibition of the endoplasmic reticulum Ca^{2+} -ATPase. *Proc Natl Acad Sci U S A* 1990; 87: 2466–2470.
- Silverstein AM, Galigniana MD, Chen MS, et al. Protein phosphatase 5 is a major component of glucocorticoid receptor hsp90 complexes with properties of an FK506-binding immunophilin. *J Biol Chem* 1997; 272: 16224–16230.
- Freichel M, Suh SH, Pfeifer A, et al. Lack of an endothelial store-operated Ca^{2+} current impairs agonist-dependent vasorelaxation in $\text{TRP4}^{-/-}$ mice. *Nat Cell Biol* 2001; 3: 121–127.

26. Pei H, Li L, Fridley BL, et al. FKBP51 affects cancer cell response to chemotherapy by negatively regulating Akt. *Cancer Cell* 2009; 16: 259–266.
27. Gassen NC, Hartmann J, Zannas AS, et al. FKBP51 inhibits GSK3[beta] and augments the effects of distinct psychotropic medications. *Mol Psychiatry* 2016; 21: 277–289.
28. Birukova AA, Birukov KG, Smurova K, et al. Novel role of microtubules in thrombin-induced endothelial barrier dysfunction. *FASEB J* 2004; 18: 1879–1890.
29. Scammell JG, Denny WB, Valentine DL, et al. Overexpression of the FK506-binding immunophilin FKBP51 is the common cause of glucocorticoid resistance in three New World primates. *Gen Comp Endocrinol* 2001; 124: 152–165.
30. Scheinman RI, Gualberto A, Jewell CM, et al. Characterization of mechanisms involved in transrepression of NF-kappa B by activated glucocorticoid receptors. *Mol Cell Biol* 1995; 15: 943–953.
31. Webster JC, Oakley RH, Jewell CM, et al. Proinflammatory cytokines regulate human glucocorticoid receptor gene expression and lead to the accumulation of the dominant negative beta isoform: a mechanism for the generation of glucocorticoid resistance. *Proc Natl Acad Sci U S A* 2001; 98: 6865–6870.
32. Oakley RH and Cidlowski JA. The biology of the glucocorticoid receptor: new signaling mechanisms in health and disease. *J Allergy Clin Immunol* 2013; 132: 1033–1044.
33. Hong H, Kohli K, Garabedian MJ, et al. GRIP1, a transcriptional coactivator for the AF-2 transactivation domain of steroid, thyroid, retinoid, and vitamin D receptors. *Mol Cell Biol* 1997; 17: 2735–2744.
34. Wozniak GM, Rüegg J, Abel GA, et al. FK506-binding proteins 51 and 52 differentially regulate dynein interaction and nuclear translocation of the glucocorticoid receptor in mammalian cells. *J Biol Chem* 2005; 280: 4609–4616.
35. Chen MS, Silverstein AM, Pratt AB, et al. The tetratricopeptide repeat domain of protein phosphatase 5 mediates binding to glucocorticoid receptor heterocomplexes and acts as a dominant negative mutant. *J Biol Chem* 1996; 271: 32315–32320.
36. Zuo Z, Urban G, Scammell JG, et al. Serine/threonine protein phosphatase type 5 (PP5) is a negative regulator of glucocorticoid receptor-mediated growth arrest. *Biochemistry* 1999; 38: 8849–8857.
37. Zhang Y, Leung DY, Nordeen SK, et al. Estrogen inhibits glucocorticoid action via protein phosphatase 5 (PP5)-mediated glucocorticoid receptor dephosphorylation. *J Biol Chem* 2009; 284: 24542–24552.
38. Bouazza B, Krytska K, Debba-Pavard M, et al. Cytokines alter glucocorticoid receptor phosphorylation in airway cells: role of phosphatases. *Am J Respir Cell Mol Biol* 2012; 47: 464–473.
39. Chatterjee A, Wang L, Armstrong DL, et al. Activated Rac1 GTPase translocates protein phosphatase 5 to the cell membrane and stimulates phosphatase activity *in vitro*. *J Biol Chem* 2009; 285: 3872–3882.
40. Kása A, Czikora I, Verin AD, et al. Protein phosphatase 2A activity is required for functional adherent junctions in endothelial cells. *Microvasc Res* 2013; 89: 86–94.
41. Ramsey AJ and Chinkers M. Identification of potential physiological activators of protein phosphatase 5. *Biochemistry* 2002; 41: 5625–5632.
42. Yamaguchi F, Umeda Y, Shimamoto S, et al. S100 proteins modulate protein phosphatase 5 function: a link between Ca^{2+} signal transduction and protein dephosphorylation. *J Biol Chem* 2012; 287: 13787–13798.
43. Ochoa CD, Alexeyev M, Pastukh V, et al. Pseudomonas aeruginosa exotoxin Y is a promiscuous cyclase that increases endothelial tau phosphorylation and permeability. *J Biol Chem* 2012; 287: 25407–25418.
44. Zhang J, Zhang Z, Brew K, et al. Mutational analysis of the catalytic subunit of muscle protein phosphatase-1. *Biochemistry* 1996; 35: 6276–6282.
45. Barik S. Immunophilins: for the love of proteins. *Cell Mol Life Sci* 2006; 63: 2889–2900.